

Characterization of friction stir consolidated recycled billet by uniaxial compression tests with miniaturized cylindrical specimen

LATIF Abdul^{1,a,*}, INGARAO Giuseppe^{1,b}, FRATINI Livan^{1,c}, HETZ Peter^{2,d}
and MERKLEIN Marion^{2,e}

¹University of Palermo, Viale delle Scienze, 90128 Palermo, Italy

²Institute of Manufacturing Technology, Friedrich-Alexander-Universität Erlangen-Nürnberg,
Egerlandstraße 13, 91058 Erlangen, Germany

^aabdul.latif@unipa.it, ^bgiuseppe.ingarao@unia.it, ^clivan.fratini@unipa.it, ^dpeter.hetz@fau.de,
^emarion.merklein@fau.de

Keywords: Aluminum Alloys, Recycling, Friction Stir Consolidation, Compression Test

Abstract. Friction stir consolidation (FSC) is a solid-state recycling method that directly converts machining scraps into semifinished billets. This process has been proven to be a more energy efficient and environmentally friendly technique compared to remelting based conventional recycling methods. During FSC, machining chips are transformed into a solid billet by the stirring action and friction heat of the rotating tool. Due to process mechanics, especially temperature gradient and strain rate, billets have shown different hardness values and grain size distribution across their sections. Therefore, in this research, miniaturized upsetting samples are extracted from the FSC billet. The purpose of minimizing the sample size is to get the local properties of a particular position. The intensive characterization was performed with future goals to find a more accurate numerical modelling and ultimately assign FSC billet to a potential industrial application.

Introduction

The current global demand for aluminum is 100 million tonnes per year [1]. The accelerating consumption, due to its growing application in lightweight transport, packaging, construction, and electronic industries, is putting immense pressure on industries to increase the production rate. However, per 1 ton of aluminum production from the primary source, 12-16 tons of greenhouse gas (GHG) are produced, which have severe adverse environmental impacts [2]. Besides, aluminum production from ores is also energy-intensive, leading to 13 Exa joules of energy consumption, and is therefore responsible for almost 1% of total global energy consumption [3].

Interestingly, aluminum is an infinitely recyclable material [3]. In Europe, almost 35 % of the aluminum demand is met by recycling aluminum scraps [4]. The conventional recycling route involves re-melting the metal, and thus it skips many of the complex steps of aluminum extraction from the primary source. Furthermore, recycling is highly energy efficient, requiring 5% of the energy compared to obtain aluminum from the primary bauxite source. Thus, recycling can shift aluminum's energy and carbon balance sustainability towards much greater sustainability.

The conventional recycling method has further limitations, especially during the recycling aluminum machining chips. The chip has a high surface-to-volume ratio and is highly oxidation prone, causing permanent material loss during the melting process. They cause adverse environmental impact, high cost, and significant permanent material loss [5]. Looking to the proportion, the machining scraps constitute almost 17% of the total scraps [6]. Therefore, the researchers turned to solid-state recycling (SSR) techniques. SSR are those methods that transform metal scraps directly into finished or semi-finished billet through mechanical means such as high pressure, friction, rotational speed, and force [7]. Recently, SSR processes have been analyzed as a potential alternative for recycling machining scraps.

Various SRR methods have been introduced for recycling metal chips based on the process mechanics and properties of desired product [8-10]. In fact, by omitting the melting phase, permanent losses mainly due to oxidation are avoided. Duflou et al. [5] have proved that equal channel angular pressing and spark plasma sintering outperform conventional remelting-based routes from the environmental impact perspective. Baffari et al. [11] proved the energy efficiency of friction stir extrusion.

Recently FSC has proved to be one of the environment recycling techniques compared to conventional remelting [12]. This technology has attracted many researchers as it proved its potential beyond the concept of recycling toward upcycling method [13]. FSC has two main steps: compaction and consolidation. During compaction, chips or powder are pressed in a hollow die chamber by applying a specific load through a cylindrical tool. Then compacted materials are further pressed and stirred through the tool's downward force and rotational speed during the consolidation phase [14]. So far, researchers numerically modelled [15] FSC process, identified the key process parameters [12] and proved its environmental efficiency with respect to conventional remelting.

A typical FSC, due to process mechanics such as different temperatures and strain rate distribution, is characterized by variation in mechanical properties along the radial and longitudinal direction of the billet [13, 14]. Previously, this variation was validated by Vickers's hardness test and grain size distribution analysis [16]. It is also crucial to analyze the effect of process mechanics on other important properties such as mechanical strength, fracture strength, and ductility. These mechanical properties can be obtained through tensile tension or compression test. However, due to variation in properties across the FSC billet section, miniaturized samples were extracted from the billet section. Interestingly, the miniaturization of the sample leads to homogenization and thus gives details of local properties. The concept of miniaturized samples for upsetting test, previously implemented by Hetz et al. [17] for sheet metal, was applied to the FSC billet. The broader objective is to find a more accurate solution for the numerical modelling of the FSC process and find the potential industrial application.

Material and methods

Material and process set-up.

As-received material was a 20x20 mm squared bar of AA 2011-T3. The bar was reduced into chips by a milling operation. The machining scraps were kept submerged in acetone for 15 minutes for efficient cleaning. An input chip mass of 15g was loaded in the cylindrical die with a nominal diameter of 25.4 mm and compacted at 5 kN force through an H13 steel cylindrical tool with a 25 mm diameter. The die and pressing tool were integrated with ESAB-LEGIO (Fig. 1), a dedicated friction stir welding machine. The chips compaction was an important step in order to avoid spilling out chips during consolidation. Finally, chips were transformed into a cylindrical billet by applying the rotating tool at 1500 rpm and 20 kN load for a processing time of 30 seconds. The selected process parameters in the current investigation were based on previous studies [13,16] as promising conditions for manufacturing sound billet.

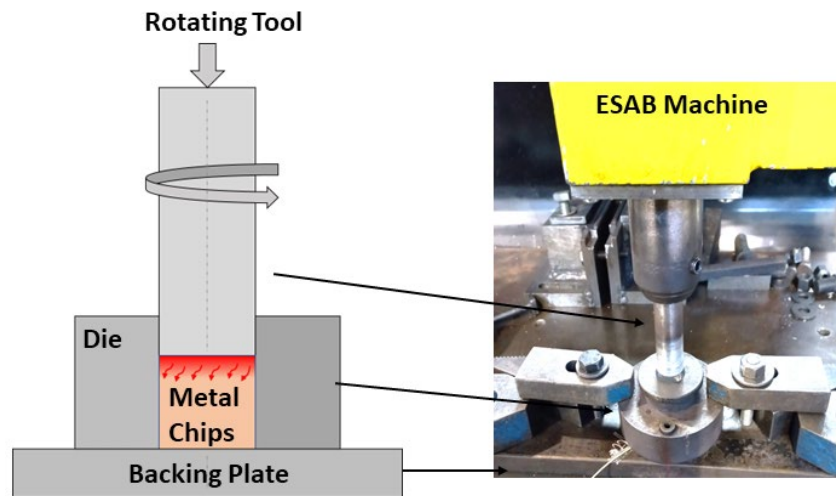


Fig. 1. Experimental setup of FSC.

Measured outputs.

After FSC consolidated step, the obtained billets had an average height and a diameter of 10 mm and 25 mm, respectively. First, the top and bottom surfaces of the FSC cylindrical billet were well polished to get a very flat surface. Then slices were cut (perpendicular to the cylindrical axis of the billet) from the top, middle, and bottom sections with a thickness of 1.5 mm and a diameter equal to the original billet diameter, as shown in Fig. 2 (right). From each disc slice, five miniaturized cylindrical upsetting samples were extracted that had a height (h) of 1.5 mm (slice thickness) and a diameter (d) of 1 mm through micro-EDM on an SX-200-HPM (Sarix SA). One sample (x1) was extracted from the center (r=0) and the remaining four samples (x2, x3, x4, and x5) were extracted at r=10 mm from the center of the billet. Upsetting tests were performed at a strain rate of 0.5%/s with upsetting sample dimensions given in Fig. 3. The height-to-diameter ratio (1.5) of the upsetting was selected based on the equation [17].

$$1 \leq \frac{h}{d} \leq 2 \tag{1}$$

According to this Eq. 1, a higher ratio exceeding the maximum limit leads to the buckling of the upsetting sample, which is considered a premature failure. On the other hand, a lower ratio emphasizes the effect of the frictional coefficient. Besides, Dionol ST V 1725-2 (MKU-Chemie GmbH) lubricant was applied to minimize friction.

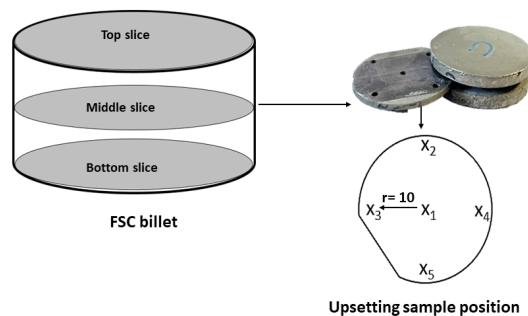


Fig. 2. Extraction of upsetting samples from FSC billet at different position.

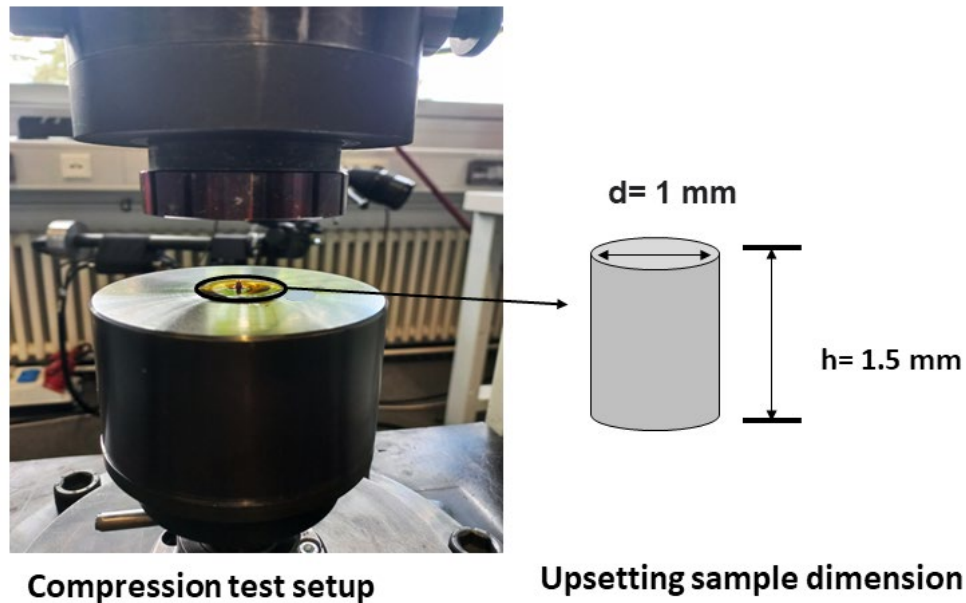


Fig. 3. Upsetting test and sample dimensions.

Results and Discussion

True-stress strain of FSC billet.

This section gives details information about the true strain-strain curves of the FSC 2011-T3 billet. It also provides evidence of how far true stress-strain graphs agree with the hardness distribution profile across the FSC billet section that the authors investigated in their previous research [13,16]. Further, a comparison was also made between the true stress-strain curve FSC recycled billet and as received AA 2011-T3 bar.

On the top slice (Fig.4), the central sample (x1) showed higher strength compared to the remaining upsetting samples (x2 to x5). The flow curves of the remaining four were found almost aligned with each other. The reason was samples x2 to x5 were extracted from the same height (top slice) and same radial distance ($r=10$ mm). Interestingly, the variation in properties is enabled by FSC process mechanics, i.e., different strain rate and temperature distributions across the billet section, as reported by Tang et al. [14]. Although, a detailed analysis has not been performed so far, it is quite clear that the die wall and back plate serve as heat sinks, reducing the temperature. Due to this, chips close to the die wall and back plate don't receive sufficient heat input and deformation to be fully recrystallized, but some bonding is, however, achieved.

Likewise, the top slice flow curves, almost the same trend was found for the middle slice. The central specimen showed higher strength than the other samples, with the exception that the x2 graph was not aligned with the x3, x4, and x5 curves. This deviation of the x2 graph was unexpected, as x2 was extracted from the same radial distance ($r=10$ mm) and the same height (middle slice). Therefore, this misalignment could be an error that occurred while manufacturing the samples.

For the bottom slice, almost uniform flow curves were found for all samples. It is well evident that the strength of the material varies both in the radial and longitudinal direction of the billet. Further, the top part of the billet shows higher strength than the bottom part, and along the radial direction the central part is stronger than the region near the external surface. Also, along the radial direction, the difference in true stress-strain curves between the samples at the center (x1) and the other samples (x2 to x5) is higher for the top slice, then difference diminishes at the middle slices, and finally, all curves are aligned with each other for the bottom slice. For better understanding,

the trend of true stress-strain curves is discussed in terms of hardness distribution in the following section.

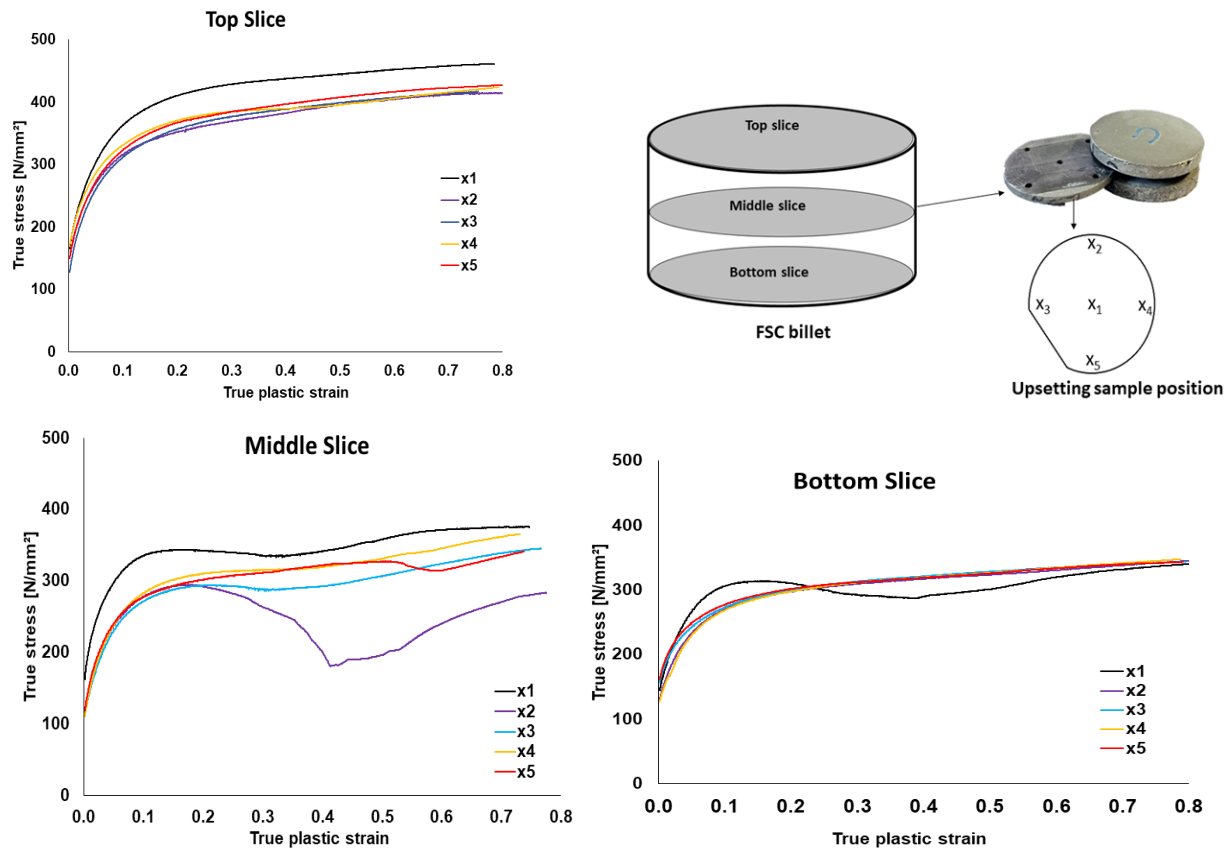


Fig. 4. True stress-strain curves for top, middle and bottom slices of FSC billet.

Comparison FSC billet true strain-strain and hardness trend.

Interestingly, the trend of true strain-strain profile was found very consistent with the hardness distribution trend. The hardness measurements were performed on the same material, AA 2011-T3, manufactured under the same process configuration as mentioned previous section. For hardness, a load of 49 N was applied for 15 seconds as dwell time.

As in Fig.5 (right side), on the top surface, the hardness value is higher, but variation in the radial direction is also very high. Similarly, in Fig.5 (left) the true stress-strain curves showed the material has good strength at the top (x1, x2, and x3), but the difference in material strength between x1 and x2/x3 is higher. It should be noted that x1 is an upsetting sample at the center (r=0), and x2 and x3 are at the left and right sides, respectively, of x1. Besides, x2 and x3 are at equidistance (r=10 mm) from x1.

Again in Fig.5 (right), the mid of the billet section shows a minor variation in hardness value along the radial direction. A similar relationship can be found for the flow curves of middle slice y1 and y2/y3 in Fig.5 (left).

For the bottom section, a lower but uniform hardness value can be noticed. Likewise, lower strengths but alignment of curves were noticed for the true stress-strain graphs of the bottom section (z1, z2, and z3).

It is quite clear that the true stress-strain curves followed the trend of hardness distribution. Overall, the central, and top zones show higher strength and higher hardness values in comparison

to the part near the external surface and bottom section, where relatively low hardness values were noticed.

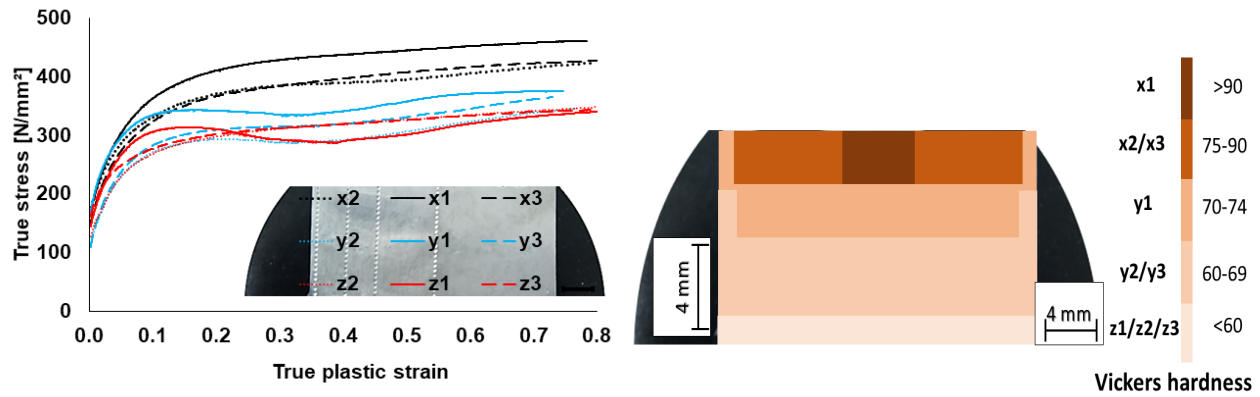


Fig. 5. Comparison between true stress-strain curves profiles and hardness distribution across FSC billet.

Comparison of true strain-strain profile of FSC billet and as-received material.

For the sake of better understanding, the true stress-strain curve of the as-received bar of AA 2011-T3 was compared with flow curves of specimens that were extracted from the center of the top (x1), middle (y1), and bottom (z1) slices of FSC billet section as shown in Fig. 6. Interestingly, the strength of the top layer of FSC billet was higher, middle slice's was comparable, and bottom slice strength was lower than as-received material. The variation in strength was previously also observed in the hardness profile. So, it is well evident that this phenomenon was enabled by FSC process mechanics [13,14, 16]. Dynamics recrystallization and full consolidation occur at the top surface, making the top surface superior to the as-received material.

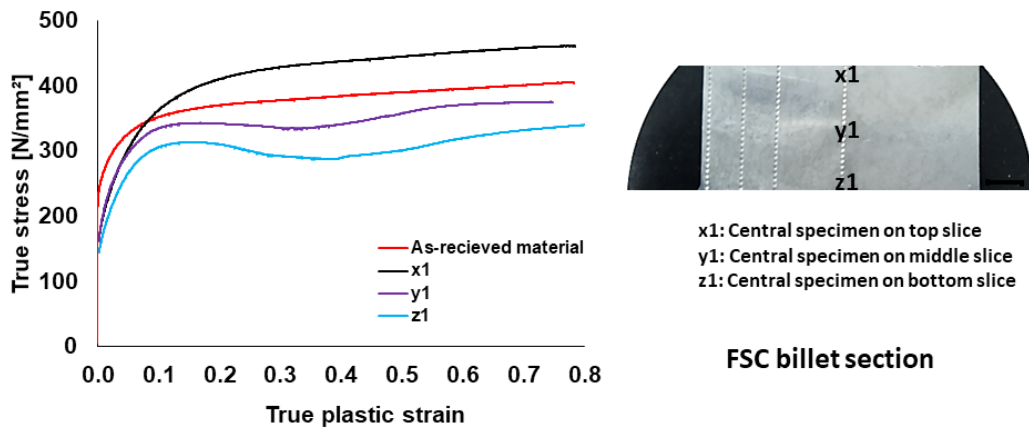


Fig. 6. Comparison of true stress-strain curve between as-received material and different section of FSC billet.

Summary

Based on the previous discussion, the following can be concluded.

1. The strength of FSC billet decreases both along billet advancing direction and radial direction.
2. The strength of top section is higher than strength of bottom section. Similarly, higher strength was found along the central part ($r=0$) compared to the strength of region near the external surface.
3. The flow curves were found in good agreement with the hardness trend across the billet section. It means that hardness is a good indicator for predicting FSC billet strength.

4. The region where the billet shows a higher hardness value also shows higher strength, and similar results were also valid for the zone of lower hardness value that showed lower strength.

It has been proved that the FSC process causes variations in the mechanical properties of the billet. The authors proved that multi-step FSC processes [16] implementation allows billet with more uniform mechanical and microstructural properties to be obtained. Further development will focus on the here presented characterization of multiple-step FSCed samples. The authors, in their previous studies [18], analyzed the performance of FSCed billets by conducting forging tests, and further developments are still in progress in terms of the double cup extrusion test. Also, an accurate numerical model will be developed in order to provide clarity on the process mechanics and to understand the actual factor causing the sample heterogeneity.

References

- [1] Information on <https://alucycle.international-aluminium.org/public-access/>
- [2] T.G. Gutowski, S. Sahni, J.M. Allwood, M.F. Ashby, E. Worrell, The energy required to produce materials: constraints on energy-intensity improvements, parameters of demand, *Philos. Trans. Royal Soc. A: Math. Phys. Eng. Sci.* 371 (2013) 20120003. <https://doi.org/10.1098/rsta.2012.0003>
- [3] D. Raabe, D. Ponge, P.J. Uggowitzer, M. Roscher, M. Paolantonio, C. Liu, H. Antrekowitsch, E. Kozeschnik, D. Seidmann, B. Gault, F. De Geuser, A. Dechamps, C.R. Hutchinson, C. Liu, Z. Li, P. Prangnell, J. Robson, P. Shanthraj, S. Vakili, C.W. Sinclair, L. Bourgeois, S. Pogatcher, Making sustainable aluminum by recycling scrap: The science of “dirty” alloys, *Progr. Mater. Sci.* (2022) 100947. <http://dx.doi.org/10.1016/j.pmatsci.2022.100947>
- [4] Information on <https://www.iea.org/reports/material-efficiency-in-clean-energy-transitions>
- [5] J.R. Duflou, A.E. Tekkaya, M. Haase, T. Welo, K. Vanmeensel, K. Kellens, W. Dewulf, D. Paraskevas, Environmental assessment of solid state recycling routes for aluminium alloys: can solid state processes significantly reduce the environmental impact of aluminium recycling?. *CIRP Annals* 64 (2015) 37-40. <https://doi.org/10.1016/j.cirp.2015.04.051>
- [6] U.M.J. Boin, M. Bertram. Melting standardized aluminum scrap: A mass balance model for Europe, *JOM* 57 (2005) 26-33. <https://doi.org/10.1007/s11837-005-0164-4>
- [7] B. Wan, W. Chen, T. Lu, F. Liu, Z. Jiang, M. Mao, Review of solid state recycling of aluminum chips, *Resources, Conservation and Recycling* 125 (2017) 37-47. <https://doi.org/10.1016/j.resconrec.2017.06.004>
- [8] M. Haase, N.B. Khalifa, A.E. Tekkaya, W.Z. Misiolek, Improving mechanical properties of chip-based aluminum extrudates by integrated extrusion and equal channel angular pressing (iECAP), *Mater. Sci. Eng. A* 539 (2012) 194-204. <https://doi.org/10.1016/j.msea.2012.01.081>
- [9] F. Widerøe, T. Welo, Using contrast material techniques to determine metal flow in screw extrusion of aluminium, *J. Mater. Process. Technol.* 213 (2013) 1007-1018. <http://doi.org/10.1016/j.jmatprotec.2012.11.013>
- [10] D. Paraskevas, S. Dadbakhsh, J. Vleugels, K. Vanmeensel, W. Dewulf, J. Duflou, Solid state recycling of pure Mg and AZ31 Mg machining chips via spark plasma sintering, *Mater. Des.* 109 (2016) 520-529. <http://doi.org/10.1016/j.matdes.2016.07.082>
- [11] D. Baffari, A.P. Reynolds, A. Masnata, L. Fratini, G. Ingarao, Friction stir extrusion to recycle aluminum alloys scraps: energy efficiency characterization, *J. Manuf. Process.* 43 (2019) 63-69. <https://doi.org/10.1016/j.jmapro.2019.03.049>
- [12] G. Buffa, D. Baffari, G. Ingarao, L. Fratini, Uncovering technological and environmental potentials of aluminum alloy scraps recycling through friction stir consolidation, *Int. J. Precis. Eng. Manuf.-Green Technol.* 7 (2020) 955-964. <https://doi.org/10.1007/s40684-019-00159-5>
- [13] A. Latif, G. Ingarao, L. Fratini, Multi-material based functionally graded billets manufacturing through friction stir consolidation of aluminium alloys chips, *CIRP Annals* 71 (2022) 261-264. <https://doi.org/10.1016/j.cirp.2022.03.035>

- [14] W. Tang, A.P. Reynolds, Friction consolidation of aluminum chips, in: *Friction Stir Welding and Processing VI*, 2011, pp. 289-298. <http://doi.org/10.1002/9781118062302.ch34>
- [15] D. Baffari, A.P. Reynolds, X. Li, L. Fratini Bonding prediction in friction stir consolidation of aluminum alloys: A preliminary study, in: *AIP Conference Proceedings 1960* (2018) p. 050002, AIP Publishing LLC.
- [16] A. Latif, G. Ingarao, M. Gucciardi, L. Fratini, A novel approach to enhance mechanical properties during recycling of aluminum alloy scrap through friction stir consolidation, *Int. J. Adv. Manuf. Technol.* 119 (2022) 1989-2005. <https://doi.org/10.1007%2Fs00170-021-08346-y>
- [17] P. Hetz, M. Kraus, M. Merklein, Characterization of sheet metal components by using an upsetting test with miniaturized cylindrical specimen, *CIRP Annals* 71 (2022) 233-236. <https://doi.org/10.1016/j.cirp.2022.03.010>
- [18] A. Latif, G. Ingarao, G. Buffa, L. Fratini, Forgeability characterization of multi-material based functionally graded materials manufactured through friction stir consolidation, in: *IOP Conference Series: Mater. Sci. Eng.* 1270 (2022) 012096. <https://doi.org/10.1088/1757-899X/1270/1/012096>